

# Microstructure and mechanical properties of Al 7075 alloy processed by differential speed rolling

Kristóf Bobor / Zoltán Hegedűs / Jenő Gubicza / István Barkai / Péter Pekker / György Krallics

Received 2012-06-30

## Abstract

Al 7075 alloy was equal and differential speed rolled according to various deformation routes. In these routes the sheets were rotated around different axes between subsequent passes of rolling. The mechanical properties and the microstructure of the specimens processed by various routes were compared. It was found that while the strength values were irrespective of the rolling routes, the ductility depends strongly on the deformation method. The differences in the mechanical behavior were explained by the edge/screw character in the dislocation structure.

## Keywords

aluminium alloys · nanostructured materials · mechanical characterization · X-ray diffraction · electron microscopy

## 1 Introduction

The reduction of grain size in polycrystalline metallic materials usually has a beneficial effect on mechanical properties resulting in high strength, low temperature of ductile-to-brittle transition or improved superplastic formability [1–4]. Severe plastic deformation (SPD) techniques are effective methods in grain refinement without producing contamination or large porosity in the ultrafine grained microstructures.

Differential speed rolling (DSR) is an SPD procedure that uses rolls with equal diameters rotating at different speeds. The application of this method results in large shear strains in metallic sheets and therefore it can be used for production of ultrafine grained metals [5–9]. An advantage of this technique is that it enables continuous production in contrast to other SPD methods such as equal channel angular pressing (ECAP) or high pressure torsion (HPT). This favourable feature of DSR has attracted large interest in recent years. Beside the grain refinement, a homogeneous and beneficial texture can be achieved by this technique, that may increase the ductility and formability of Al [10], Ti [11] and Mg [12–14] alloys. The texture developed by DSR was investigated by several authors.

The four different routes of DSR are illustrated in Fig. 1 [15, 16]. In the case of route UD no rotation of the sample occurs, whereas for routes ND, RD, and TD the sample is rotated by 180° around the normal, the rolling and the transverse axes, respectively. The grain structure and the through-thickness texture gradient produced by the different routes of DSR have been studied in Al 1050 aluminium alloy [15, 16]. It was found that DSR gives rise to the shear textures through the thickness which are closer to the ideal shear texture if they are obtained by changes in the shear direction. In a recently published paper [17], the DSR method was compared with other SPD techniques in terms of monotony of deformation. It was established that the monotony of DSR is close to those of ECAP and HPT methods yielding a similar effectiveness in grain refinement. The aim of the present work is to investigate the effect of the various DSR routes on the microstructure and mechanical properties of Al 7075 aluminium alloy.

## Kristóf Bobor

Department of Materials Science and Engineering, BME, 1111 Budapest, Bertalan Lajos u. 3., Hungary  
e-mail: kristof.bobor@gmail.com

## Zoltán Hegedűs

## Jenő Gubicza

Department of Materials Physics, Eötvös Loránd University, H-1117, Budapest, Pázmány Péter Sétány 1/A, Hungary

## István Barkai

## Péter Pekker

## György Krallics

Bay Zoltán Foundation for Applied Research, Institute for Nanotechnology, H-1116 Budapest, Fehérvári út 130., Hungary

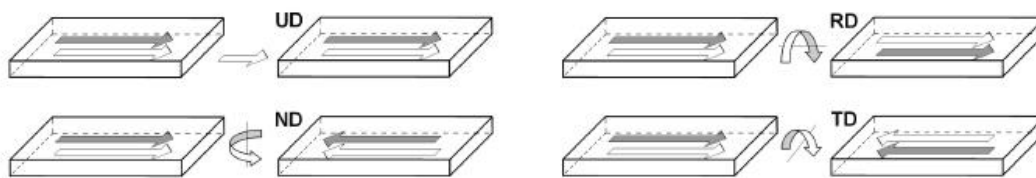


**Fig. 1.** Various routes of DSR. In the case of UD the specimen is not rotated, whereas in RD, TD, and ND routes the specimen is rotated by 180° around the RD, TD and ND axes, respectively.

**Tab. 1.** Chemical composition of Al 7075 alloy (in weight percent)

Al	Zn	Mg	Cu	Cr	Fe	Si	Mn	Ti
88–92	5.1–6.1	2.1–2.9	1.2–2.0	0.18–0.28	max 0.50	max 0.40	max 0.3	max 0.20

**Tab. 2.** The thickness reductions during various passes of DSR

	1. pass	2. pass	3. pass	4. pass
Initial thickness (mm)	10	7	5	3.5
Rolled thickness (mm)	7	5	3.5	2.5
Reduction (%)	30	28	30	28

**Tab. 3.** The area-weighted mean crystallite size ( $\langle x \rangle_{area}$ ), the dislocation density ( $\rho$ ) and the parameter  $q$  characterizing the edge or screw character of the dislocation structure determined by X-ray line profile analysis.

	$\langle x \rangle_{area}$ (nm)	$\rho$ ( $10^{14} \text{ m}^{-2}$ )	$q$
ESR, UD100	102±10	4.8±0.5	0.63±0.05
DSR, UD40	108±10	5.5±0.5	0.60±0.05
DSR, ND40	107±10	5.5±0.5	0.51±0.05
DSR, RD40	86±9	4.3±0.5	0.38±0.05
DSR, TD40	82±9	3.4±0.4	0.36±0.05

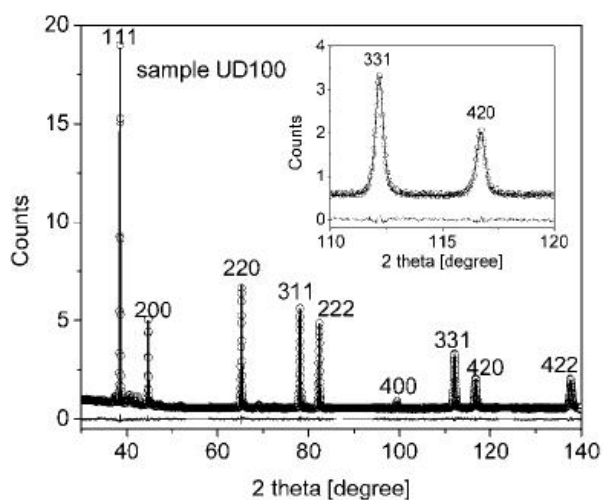


**Fig. 2.** Fitting of the X-ray diffraction pattern obtained for sample UD100 processed by ESR. The open circles and the solid line represent the measured data and the fitted curves, respectively. The difference between the measured and fitted data is also plotted at the bottom of the figure. The inset shows a part of the diffractogram with higher magnification.

## 2 Experimental details

Al 7075 alloy specimens were processed by equal speed rolling (ESR) and DSR using various rolling routes at room temperature. The chemical composition of the alloy is presented in Tab. 1.

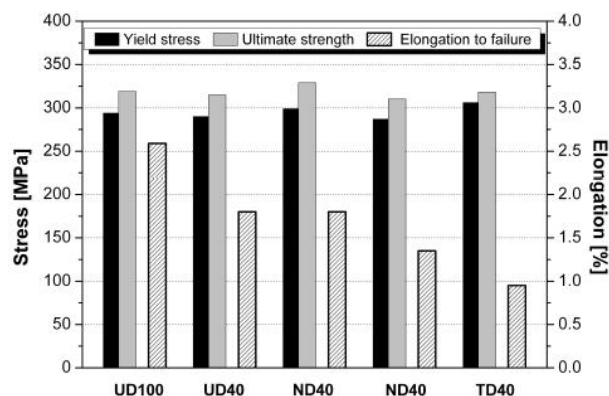


**Fig. 3.** Mechanical properties of ESR- (UD100) and DSR-processed (UD40, ND40, RD40, TD40) specimens.  $R_{p0.2}$  – yield stress,  $R_m$  – ultimate strength,  $A$  – elongation to failure

Specimens with the dimensions of  $10 \times 40 \times 150 \text{ mm}^3$  were annealed at 450°C for 2 hours and subsequently furnace cooled before rolling. The diameter of the rolls was 140 mm. In the case of ESR, the speed of both rolls was 10 rev/min while during DSR the speeds of the two rolls were different: 10 and 4 rev/min. The specimens were rolled in four passes to the final thickness of 2.5 mm. The values of thickness reduction are listed for each pass in Tab. 2. The specimens were rolled using five different routes. The specimen processed by ESR is denoted as UD100. UD40, RD40, TD40 and ND40 denote DSR accord-

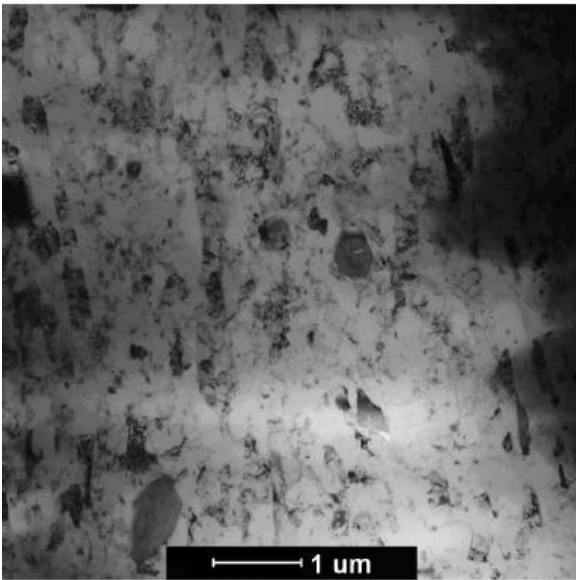


Figure 4. a)

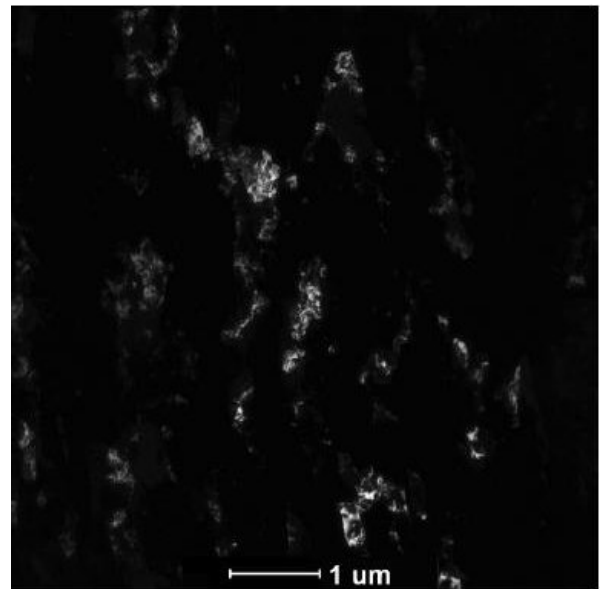


Figure 4. b)

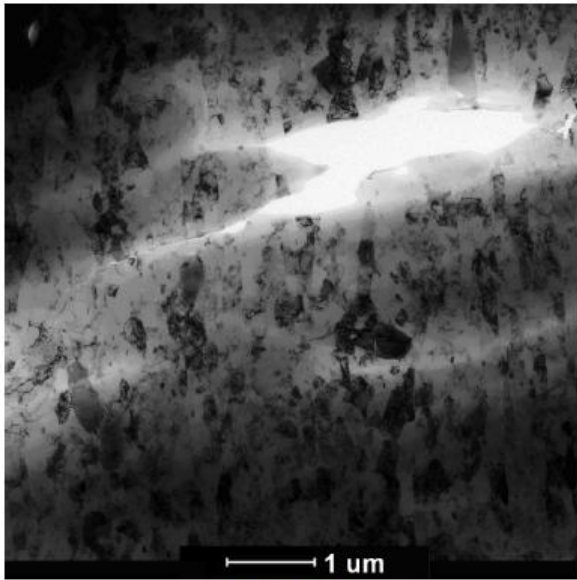


Figure 4. c)

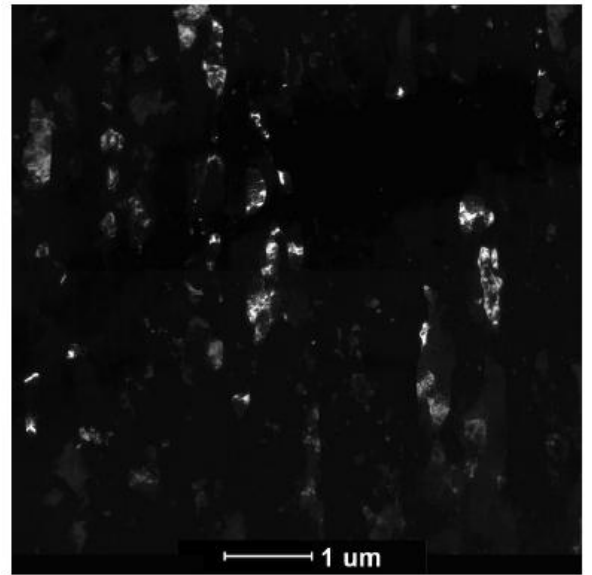


Figure 4. d)

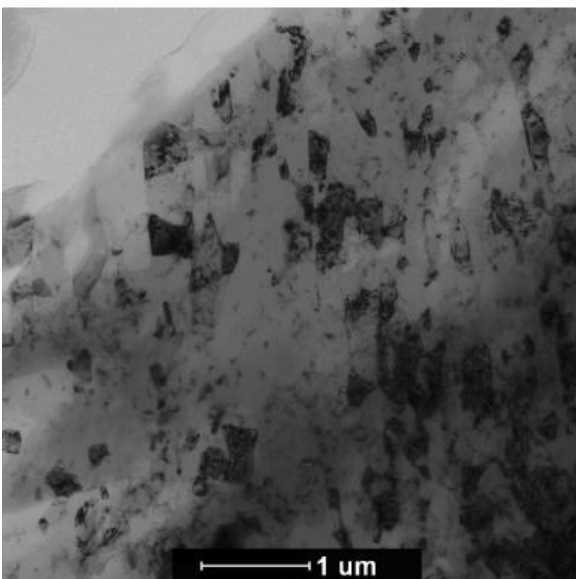


Figure 4. e)

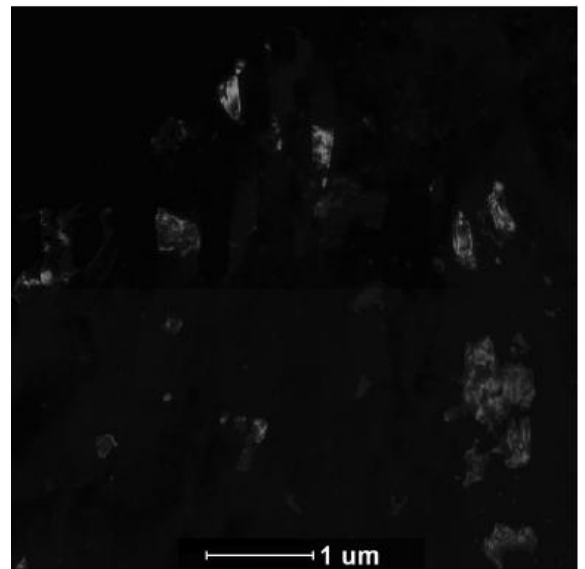


Figure 4. f)

Fig. 4. Bright and dark field TEM images of the microstructures for UD100 (a, b), UD40 (c,d) and TD40 (e,f) samples.

ing to the four different routes shown in Fig. 1. No lubricant was applied during rolling. Heat treatment was not carried out on the rolled specimens before the study of the microstructure and the mechanical behavior.

The samples for tensile test were prepared in the rolling direction of the sheets. The tensile tests were performed by an MTS 810 universal mechanical testing machine with constant cross head velocity (2 mm/s) at room temperature.

The microstructure of the rolled samples were studied by a Fei-Technai  $G^2$  type transmission electron microscope (TEM) operating at 200 kV. The TEM specimens were prepared in the plane perpendicular to the rolling direction by mechanical thinning and subsequent precision ion polishing till perforation. Moreover, TD40 sample was studied by scanning transmission electron microscope (STEM) technique on the same equipment.

The rolled samples were electropolished and the microstructure was studied by X-ray line profile analysis. The X-ray line profiles were measured by a special high-resolution diffractometer (Nonius FR591) with  $\text{CuK}\alpha_1$  radiation ( $\lambda=0.15406$  nm) in the centre of the cross section of the sheets. The X-ray line profiles were evaluated by the Convolutional Multiple Whole Profile (CMWP) fitting method [18]. In this method, the experimental pattern is fitted by the convolution of the instrumental pattern and the theoretical size and strain line profiles. The theoretical profile functions used in this fitting procedure are calculated on the basis of a model of the microstructure, where the crystallites have spherical shape and log-normal size distribution, and the lattice strains are assumed to be caused by dislocations. As an example, the fitting for the sample processed by ESR is shown in Fig. 2. The open circles and the solid line represent the measured data and the fitted curves, respectively. The difference between the measured and fitted data is also plotted at the bottom of the figure. The area-weighted mean crystallite size ( $\langle x \rangle_{area}$ ), the dislocation density ( $\rho$ ) and the parameter  $q$  characterizing the edge or screw character of the dislocation structure were determined from the fitting and listed in Tab. 3. The value of  $\langle x \rangle_{area}$  is calculated as  $\langle x \rangle_{area} = m \times \exp(2.5\sigma^2)$ , where  $m$  and  $\sigma$  are the median and the lognormal variance of the size distribution of crystallites. The parameter  $q$  was also obtained from the fitting that characterizes the type of dislocations: edge or screw or mixed. In the case of Al for pure edge and screw dislocations the values of  $q$  are 0.36 and 1.33, respectively. For a dislocation structure having mixed character the value of  $q$  is between these limiting cases.

### 3 Results and discussion

The yield and tensile strength values as well as the elongation to failure for UD100, UD40, RD40, TD40 and ND40 samples were determined from the tensile stress-strain data and plotted in Fig. 3. The yield and tensile strength values were around 300 and 320 MPa, respectively. The results show that the strength increment due to rolling is nearly independent of the type of the rolling and the DSR routes. In contrast to this, the elongation to

failure shows relatively large differences. The ESR-processed material was the most ductile, while the specimens deformed by DSR exhibited lower elongation to failure. The samples produced by routes UD and ND have the highest ductility among the ESR-processed samples. The routes RD and TD resulted in significantly lower ductility than routes UD and ND. The smallest elongation to failure was under one percent as obtained for the sample processed by route TD.

Selected TEM images for samples UD100, UD40 and TD40 can be seen in Fig. 4. Contrary to the various ductility of these samples, the TEM results show no significant differences between the microstructures. The average grain size was 400-500 nm for all the studied samples. The SEM image in Fig. 5 shows a precipitated microstructure in sample TD40. The precipitates were identified by X-ray diffraction as hexagonal  $\text{MgZn}_2$  ( $\eta'/\eta$  precipitates). The X-ray diffraction patterns did not reveal differences in the structure and size of precipitates in the samples processed by various routes of rolling.

The mean crystallite size and the dislocation density obtained by X-ray diffraction line profile analysis can be seen in Tab. 3. The results show that the samples produced by routes RD and TD of DSR have slightly smaller crystallite size and lower dislocation density than in the specimens processed by routes UD and ND or by ESR. The character of dislocations is rather edge for all the studied samples as revealed by the values of  $q$  parameter that are smaller than the arithmetic average (0.85) of the  $q$  values calculated for pure edge and screw cases (see Tab. 3). The edge character of the dislocation structure is stronger for the specimens produced by routes RD and TD than in the samples processed by routes UD and ND or by ESR. This experimental evidence can explain the smaller ductility of the former samples as follows.

The Al-7xxx alloys usually contain Guinier-Preston (GP) zones and/or  $\eta'/\eta$  precipitates. These precipitates hinder dislocation glide beside other obstacles such as grain boundaries and Lomer-Cottrell locks. During deformation dislocation pile-ups form at these glide obstacles and the high stresses emerging at pile-ups are often responsible for crack initiation that may yield failure of the sample. Screw or edge dislocations captured in pile-ups can escape by cross-slip or climb mechanism, respectively. As during deformation at room temperature cross-slip occurs much easier than climb, therefore the plasticity is less obstructed by the glide obstacles if the dislocation structure has rather screw character. For the studied samples, the stronger edge character of dislocations in the specimens processed by asymmetric RD and TD routes may explain the smaller ductility of these samples.

### 4 Conclusions

In the present study Al 7075 alloy was symmetrically and asymmetrically rolled according to different deformation routes. The effect of the rolling route on the microstructure and the mechanical properties were investigated. The results can be sum-

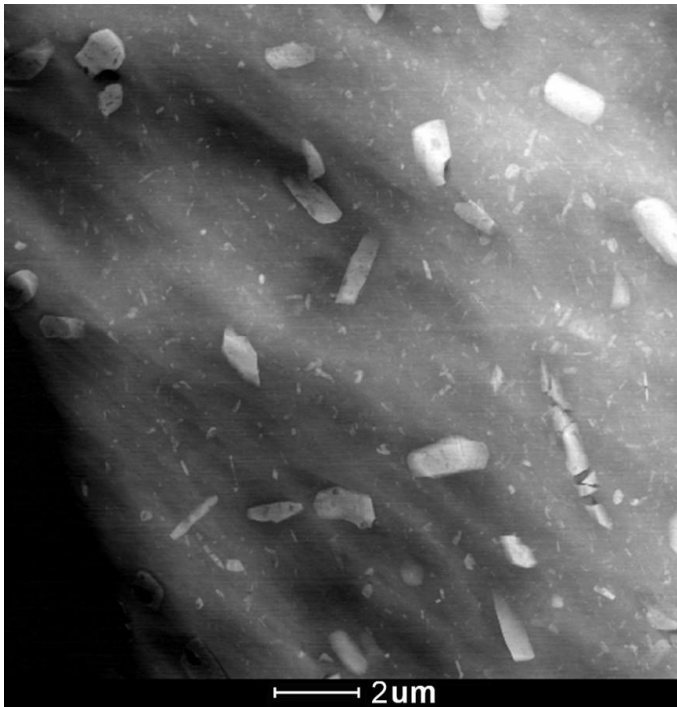


Fig. 5. STEM image of the microstructure for TD40 sample.

marized as follows:

- 1 Both yield and tensile strength values were irrespective of the rolling routes.
- 2 At the same time, the ductility showed significant differences for the samples processed by various ways of rolling. The sample processed by ESR exhibited the highest ductility. Among the asymmetrically rolled specimens, routes RD and TD yielded lower elongation to failure than routes UD and ND.
- 3 The differences in ductility were explained by the variation of the edge/screw character of the dislocation structure. The stronger edge character resulted in more difficult escape of dislocations from pile-ups leading to easier cracking during tensile testing.

### Acknowledgement

This work was supported by Bay Zoltán Foundation for Applied Research Institute for Nanotechnology (BAY-NANO). JG is grateful for the financial support of the Hungarian Scientific Research Fund, OTKA, Grant No. K-81360. The European Union and the European Social Fund have provided financial support to this project under grant agreement no. TÁ-MOP 4.2.1./B-09/1/KMR-2010-0003. The authors would like to thank I. Orbulov and K. Májlínger for the help given on the mechanical testing.

### References

- 1 Valiev RZ, Islamgaliev RK, Alexandrov IV, *Bulk nanostructured materials from severe plastic deformation*, Prog. Mater. Sci **45** (2000), 103–189, DOI 10.1016/S0079-6425(99)00007-9.

- 2 Zhu YT, Lowe TC, Langdon TG, *Performance and applications of nanostructured materials produced by severe plastic deformation*, Scripta Mater **51** (2004), 825–830, DOI 10.1016/j.scriptamat.2004.05.006.
- 3 Xu Ch, Furukawa M, Horita Z, Langdon TG, *Severe plastic deformation as a processing tool for developing superplastic metals*, J. Alloy Compd **378** (2004), 27–34, DOI 10.1016/j.jallcom.2003.10.065.
- 4 Zhang Y, Ganeev AV, Wang JT, Liu JQ, Alexandrov IV, *Observations on the ductile-to-brittle transition in ultrafine-grained tungsten of commercial purity*, Mat. Sci. Eng. A-Struct **503** (2009), 37–40, DOI 10.1016/j.msea.2008.07.074.
- 5 Ding Y, Jiang J, Shan A, *Microstructures and mechanical properties of commercial purity iron processed by asymmetric rolling*, Mat. Sci. Eng. A **509** (2009), 76–80, DOI 10.1016/j.msea.2009.01.062.
- 6 Jiang J, Ding Y, Zuo F, Shan A, *Mechanical properties and microstructures of ultrafine-grained pure aluminum by asymmetric rolling*, Scripta Mater **60** (2009), 905–908, DOI 10.1016/j.scriptamat.2009.02.016.
- 7 Lee JB, Konno TJ, Jeong HG, *Grain refinement and texture evolution in AZ31 Mg alloys sheet processed by differential speed rolling*, Mat. Sci. Eng. B **161** (2009), 166–169, DOI 10.1016/j.mseb.2009.02.021.
- 8 Kim WJ, Wang JY, Choi SO, Choi HJ, Sohn HT, *Synthesis of ultra high strength Al-Mg-Si alloy sheets by differential speed rolling*, Mat. Sci. Eng. A **520** (2009), 23–28, DOI 10.1016/j.msea.2009.05.010.
- 9 Zuo F, Jiang J, Shan A, Fang J, Zhang X, *Shear deformation and grain refinement in pure Al by asymmetric rolling*, T. Nonferr.Metal. Soc **18** (2008), 774–777, DOI 10.1016/S1003-6326(08)60133-8.
- 10 Jin H, Lloyd DJ, *Effect of a duplex grain size on the tensile ductility of an ultra-fine grained Al-Mg alloy, AA5754, produced by asymmetric rolling and annealing*, Scripta Mater **50** (2004), 1319–1323, DOI 10.1016/j.scriptamat.2004.02.021.
- 11 Huang X, Suzuki K, Chino Y, *Influences of initial texture on microstructure and stretch formability of Mg-3Al-1Zn alloy sheet obtained by a combination of high temperature and subsequent warm rolling*, Scripta Mater **63** (2010), 473–476, DOI 10.1016/j.scriptamat.2010.04.032.
- 12 Jeong HG, Jeong YG, Kim WJ, *Microstructure and superplasticity of AZ31 sheet fabricated by differential speed rolling*, J.Alloy Compd **483** ((2009)), 279–282, DOI 10.1016/j.jallcom.2008.08.130.
- 13 Kim WJ, Park JD, Kim WY, *Effect of differential speed rolling on microstructure and mechanical properties of an AZ91 magnesium alloy*, J. Alloy Compd **460** (2008), 289–293, DOI 10.1016/j.jallcom.2007.06.050.
- 14 Watanabe H, Mukai T, Ishikawa K, *Effect of temperature of differential speed rolling on room temperature mechanical properties and texture in an AZ31 magnesium alloy*, J. Mater. Proc. Tech **182** (2007), 644–647, DOI 10.1016/j.jmatprotec.2006.08.010.
- 15 Lee JK, Lee DN, *Texture control and grain refinement of AA1050 Al alloy sheets by asymmetric rolling*, Int. J. Mech. Sci **50** (2008), 869–887, DOI 10.1016/j.ijmecsci.2007.09.008.
- 16 Lee JK, Lee DN, *Texture Evolution and Grain Refinement in AA1050 Aluminum Alloy Sheets Asymmetrically Rolled with Varied Shear Directions*, Key Eng. Mat **340–341** (2007), 619–626, DOI 10.4028/www.scientific.net/KEM.340-341.619.
- 17 Bobor K, Krallics G., *Characterization of Severe Plastic Deformation Techniques with Respect to Non-Monotony*, Rev. Adv. Mater. Sci **25** (2010), 32–41.
- 18 Ribárik G, Gubicza J, Ungár T, *Correlation between strength and microstructure of ball-milled Al-Mg alloys determined by X-ray diffraction*, Mater. Sci. Eng. A **387–389** (2004), 343–347, DOI 10.1016/j.msea.2004.01.089.